NeuroImage: Clinical 31 (2021) 102709

Contents lists available at ScienceDirect

NeuroImage: Clinical

journal homepage: www.elsevier.com/locate/ynicl

Intra- and inter-hemispheric structural connectome in agenesis of the corpus callosum

Minghui Shi [a,b,1], Lorena G.A. Freitas [a,b,1], Megan M. Spencer-Smith [f,k], Valeria Kebets [b,m], Vicki Anderson [e,f,i,j], Alissandra McIlroy [f], Amanda G. Wood [f,g,h], Richard J. Leventer [c,d,e], Dimitri Van De Ville [a,b], Vanessa Siffredi [a,b,f,l,*]

[a] Institute of Bioengineering, Ecole Polytechnique Fédérale de Lausanne, Switzerland
[b] Department of Radiology and Medical Informatics, University of Geneva, Geneva, Switzerland
[c] Department of Paediatrics, University of Melbourne, Melbourne, Australia
[d] Department of Neurology, Royal Children's Hospital, Melbourne, Australia
[e] Neuroscience Research, Clinical Sciences, Murdoch Children's Research Institute, Melbourne, Australia
[f] Brain and Mind Research, Clinical Sciences, Murdoch Children's Research Institute, Melbourne, Australia
[g] School of Life and Health Sciences Aston Neuroscience Institute, Aston University, Birmingham B4 7ET, UK
[h] School of Psychology, Faculty of Health, Melbourne Burwood Campus, Deakin University, Geelong, Victoria, Australia
[i] School of Psychological Sciences, University of Melbourne, Melbourne, Australia
[j] Department of Psychology, Royal Children's Hospital, Melbourne, Australia
[k] Turner Institute for Brain and Mental Health, School of Psychological Sciences, Monash University, Melbourne, Australia
[l] Division of Development and Growth, Department of Paediatrics, Faculty of Medicine, University of Geneva, Switzerland
[m] Department of Electrical and Computer Engineering, Centre for Sleep and Cognition, Clinical Imaging Research Centre, N.1 Institute for Health, National University of Singapore, Singapore

ARTICLE INFO

Keywords:
Agenesis of the corpus callosum
Structural connectome
Graph metrics
Brain plasticity

ABSTRACT

Agenesis of the corpus callosum (AgCC) is a congenital brain malformation characterized by the complete or partial failure to develop the corpus callosum. Despite missing the largest white matter bundle connecting the left and right hemispheres of the brain, studies have shown preserved inter-hemispheric communication in individuals with AgCC. It is likely that plasticity provides mechanisms for the brain to adjust in the context of AgCC, as the malformation disrupts programmed developmental brain processes very early on. A proposed candidate for neuroplastic response in individuals with AgCC is strengthening of intra-hemispheric structural connections. In the present study, we explore this hypothesis using a graph-based approach of the structural connectome, which enables intra- and inter-hemispheric analyses at multiple resolutions and quantification of structural characteristics through graph metrics. Structural graph metrics of 19 children with AgCC (13 with complete, 6 with partial AgCC) were compared to those of 29 typically developing controls (TDC). Associations between structural graph metrics and a wide range of neurobehavioral outcomes were examined using a multivariate data-driven approach (Partial Least Squares Correlation, PLSC). Our results provide new evidence suggesting structural strengthening of intra-hemispheric pathways as a neuroplastic response in the acallosal brain, and highlight regional variability in structural connectivity in children with AgCC compared to TDC. There was little evidence that structural graph properties in children with AgCC were associated with neurobehavioral outcomes. To our knowledge, this is the first report leveraging graph theory tools to explicitly characterize whole-brain intra- and inter-hemispheric structural connectivity in AgCC, opening avenues for future research on neuroplastic responses in AgCC.

* Corresponding author.
E-mail address: vanessa.siffredi@unige.ch (V. Siffredi).
[1] These authors contributed equally to this work.

https://doi.org/10.1016/j.nicl.2021.102709
Received 22 April 2021; Accepted 25 May 2021
Available online 5 June 2021

1. Introduction

Agenesis of the corpus callosum (AgCC) is a congenital brain malformation in which the corpus callosum – the largest white matter tract bridging the left and right hemispheres of the brain– fails to develop either completely (i.e., complete AgCC) or partially (i.e., partial AgCC). The corpus callosum plays an essential role in the transmission of sensory, motor, and higher level cognitive information between homotopic regions of the two cerebral hemispheres. Individuals with AgCC have heterogeneous clinical and neurobehavioral outcomes, ranging from asymptomatic to cognitive impairment of various severity (Paul et al., 2007; Siffredi et al., 2018). This heterogeneity is thought to be partly explained by individual differences in structural neuroplasticity (Siffredi et al., 2021a).

Neuroplasticity refers to the central nervous system's capacity to dynamically modify its neural circuitry in response to the environment and experience (Anderson et al., 2011; Dennis et al., 2013). Developmental neural plasticity plays an important role in AgCC. This is evidenced by individuals born with a developmental absence of the corpus callosum showing few symptoms of inter-hemispheric disconnection syndrome, in contrast to split-brain patients who have undergone callosotomy later in life (Paul, 2011; Mancuso et al., 2019). One way of exploring neuroplasticity in these atypically developing brains is by analyzing structural connectivity.

In individuals with AgCC, structural connectivity has been explored using fiber tractography (FT) and diffusion tensor imaging (DTI). While Bénézit and colleagues (2015) showed preserved overall organization of the main white matter bundles in children with AgCC, local atypical structural organization was also observed (Bénézit et al., 2015). Studies have also reported local changes in white matter connectivity of the anterior and posterior commissures in individuals with AgCC. These changes have been hypothesized as alternative pathways for inter-hemispheric transfer of information to circumvent the absence of callosal fibers (Tovar-Moll et al., 2014; Siffredi et al., 2019). The use of connectomics approaches has also advanced our understanding of the structural organization in individuals with AgCC. Using graph theoretic metrics on the whole-brain structural connectome, Owen and colleagues (2013), and Meoded and colleagues (2015) reported reduced whole-brain global connectivity but increased local connectivity in small samples of individuals with complete AgCC compared with healthy controls (Owen et al., 2013; Meoded et al., 2015). Recently, however, analyzing structural connectivity data within and across hemispheres, Siffredi and colleagues (2021) reported a pattern of decreased inter-hemispheric but increased intra-hemispheric structural connectivity in a cohort of children with AgCC compared with typically developing controls (Siffredi et al., 2021a). Consistent with these results, Yuan and colleagues (2020) showed an increase in intra-hemispheric structural connectivity in children with AgCC associated with better verbal learning and long-term memory, verbal working memory, as well as executive and attentional functioning (Yuan et al., 2020). Notably, these findings are all in line with the previously proposed hypothesis of structural strengthening of intra-hemispheric pathways as a neuroplastic response in the acallosal brain (Chiarello, 1980; Dennis, 1976).

Given these previous findings, it is of interest to explore intra- and inter-hemispheric structural connectivity in AgCC using graph metrics. This approach can provide a clearer understanding of structural organization occurring at different scales, as well as mechanisms associated with strengthening of intra-hemispheric pathways in AgCC. Using graph theoretic metrics of the structural connectome, our study aimed to explore intra- and inter-hemispheric structural organization in children with AgCC. As an initial step, we aimed to replicate the findings of Owen and colleagues (2013) in a larger developmental cohort using the same methodology and extracting similar graph metrics and modularity measures. Secondly, we analyzed graph metrics at the network, lobe and node levels to explore intra-hemispheric and inter-hemispheric structural organization in AgCC compared to typically developing children. Lastly, we explored the association of intra- and inter-hemispheric graph metrics properties with neurobehavioral outcomes in this clinical population in comparison to typically developing controls. Comparing with existing studies that employ graph theoretical tools for structural connectome analyses in individuals with AgCC, our study sets itself apart by not only looking at whole-brain data, but also analyzing the intra- and inter-hemispheric data on three different scales (network, lobe, and node levels), as well as exploring the associations between graph metrics derived from structural connectivity and neurobehavioral measures.

2. Methods

2.1. Sample

This study used data from the "Paediatric Agenesis of the Corpus Callosum Project" conducted at the Murdoch Children's Research Institute (Siffredi et al., 2018), which examined neurobehavioral, neurological, and neuroimaging outcomes in a cohort of children with AgCC compared with typically developing children. A cohort of 28 children with AgCC, including both complete and partial AgCC, was recruited from clinics and radiology records at The Royal Children's Hospital (RCH), Melbourne. Inclusion criteria were: 1) aged 8 years 0 months to 16 years and 11 months; 2) evidence of AgCC on MRI conducted as part of a routine clinical work-up; 3) English speaking; and 4) functional ability to engage in the assessment procedure. MRI findings were qualitatively reviewed by a pediatric neurologist with expertise in brain malformations (RJL), who confirmed the diagnosis of AgCC, including complete or partial AgCC, and identified isolated or complex (i.e., associated brain malformations) AgCC. A typically developing control (TDC) group of 30 children comparable in age and sex to the AgCC group was recruited from the community.

Children were included in the study if they had completed the required MRI sequences (T1 and diffusion-weighted imaging), resulting in the exclusion of five participants from the AgCC group and one participant from the TDC group. After quality checking the diffusion MR images, two AgCC participants were excluded. Additionally, one child with AgCC was excluded due to difficulties characterizing corpus callosum malformation and one AgCC participant was excluded due to mediocre parcellation that could potentially bias the results at the node level. Seven children were assessed on two separate occasions, and for these children the most complete of the two neurobehavioral assessments was used, as well as the MRI scan completed at the time of the most complete neurobehavioral assessment. The final sample size for the graph metrics analysis was 19 children with AgCC and 29 TDC.

2.2. Procedure

This project was approved by the RCH Human Research Ethics Committee. Caregivers provided written informed consent prior to participation. Consenting families were seen at a research clinic at the Murdoch Children's Research Institute.

2.3. Material

2.3.1. Neuroimaging measures

Magnetic Resonance Imaging acquisition. Images were acquired on a 3 T MAGNETOM Trio scanner (Siemens, Erlangen, Germany) at the RCH. A 32-channel head coil was used for transmission and reception of radio-frequency and signals. A high-resolution 3D anatomical images was acquired using a T1-weighted MP-RAGE sequence (TR = 1900 ms, TE = 2.71 ms, TI = 900 ms, FA = 9°, FoV = 256 mm, voxel size = 0.7 × 0.7 × 0.7 mm). Echo planar diffusion-weighted imaging (DWI) data were acquired at two different b-values, including two scans without diffusion weighting (b-factor = 0): a) b-value = 1000 s/mm2, 30 gradient directions where 64 slices with isotropic voxels of 2 mm3 were obtained (TR = 8600 ms; TE = 90 ms; FoV = 256 mm) in an anterior to posterior

direction; and b) b-value = 3000 s/mm2, 50 gradient directions where 54 slices with isotropic voxels of 2.3 mm3 were obtained (TR = 8200 ms; TE = 112 ms; FoV = 240 mm) in an anterior to posterior direction.

Structural MRI data preprocessing. Diffusion weighted imaging (DWI) scans were converted from the native DICOM to NIFTI format using the dcm2nii tool developed at the McCauseland Centre for Neuroimaging (http://www.mccauslandcenter.sc.edu/mricro/mricron/dcm2nii.html). Each image was visually checked gradient by gradient and slice by slice. DWI data sets were pre-processed for tractography using MRtrix (Tournier et al., 2019). DWI data denoising, eddy current-induced distortion correction, motion correction and bias field correction were performed on the two different shells independently (b = 1000 and b = 3000). In order to remove non-brain tissue components and background noise, b0 images for the two shells were extracted using Brain Extraction Tool (BET2) compiled in FSL (Smith, 2002). Images from the two shells were then coregistered using FreeSurfer taking the b = 1000 shell as a reference and merged using FSL. An in-house global normalization procedure of the two DWI shell data was performed by using a normalized factor as a ratio k (k = meanb0 b = 1000 / meanb0 b = 3000) (Obertino et al., 2018). Tractography and connectome reconstruction were done using MRtrix. The Tax algorithm was used for response function estimation (Tax et al., 2014). The second order integration over fiber orientation distributions (iFOD2) algorithm was estimated using constrained spherical deconvolution with default parameters (Tournier et al., 2008). Probabilistic tractograms of one million streamlines were generated over the entire brain, with subsequent filtering to 100 thousand streamlines using Spherical Deconvolution Informed Filtering of Tractograms (SIFT) to improve the accuracy of the reconstructed whole-brain connectome (Smith et al., 2013). For each participant, the structural connectome matrix was generated from the resulting tractography using the registered Brainnetome Atlas (Fan et al., 2016). 246 × 246 connectivity matrices were obtained for each participant using the number of streamlines connecting each region of the atlas.

Study replication analyses and graph metrics extraction. In order to have a comparable sample to Owen et al. (2013), which comprised individuals with complete AgCC, we only used the structural connectome data from children with complete AgCC (n = 13) and from TDC (n = 29) in the initial replication analyses.

An unweighted consensus structural connectome was first generated for each group. The method in Grayson et al. (2014) was adopted because its structural connectivity dataset has a parcellation resolution close to that of the current dataset. For the consensus, structural connectome, only connections that existed in at least 50% of the subjects in a group were retained and the resulting connectivity matrix was binarized. The following graph metrics were then calculated: mean degree, cost, characteristic path length, mean normalized betweenness, global efficiency, local efficiency, and mean clustering coefficient. The same graph metrics were also calculated for individual structural connectivity matrices in the two groups.

Graph metrics used in the present study are defined below (Bullmore and Bassett, 2011; Owen et al., 2013):

- **Degree:** number of connections of a node. Networks with higher mean degree have denser connections.
- **Normalized betweenness:** number of shortest paths that pass through a node, after normalizing the result to one in the case of all shortest paths between all pairs of nodes in the network passing through the node of interest. Networks with higher mean normalized betweenness have more centralized shortest paths.
- **Characteristic path length:** Average length of the shortest paths between all pairs of nodes in a network. Networks with a lower characteristic path length can transmit information more quickly.
- **Global efficiency:** Mean inverse path length between all pairs of nodes. This metric is similar to the characteristic path length but less affected by extreme path lengths. Higher global efficiency is related to quicker information transfer across networks.
- **Local efficiency:** Mean inverse of the shortest path length between all nodes passing through the connected neighbors of a node. This metric represents the efficiency of information transfer in the local environment of a node.
- **Cost:** Ratio between number of suprathreshold edges and total number of possible edges in a network. Networks with higher cost have higher fiber density.
- **Clustering coefficient:** Ratio of closed triangles between triplets of nodes and number of connected triplets. Networks with a higher clustering coefficient have more nodes with inter-connected neighbors, thus enabling more efficient local integration of information.

Both degree and normalized betweenness were calculated on a node-by-node basis, while mean degree and mean normalized betweenness were obtained by averaging across all nodes either in the consensus structural connectome or in every individual connectome.

Metrics of modularity analyses, performed on both consensus and individual connectomes of complete AgCC and TDC groups, are defined below (Owen et al., 2013; Rubinov and Sporns, 2010):

- **Modularity:** The difference between the fraction of the edges that fall within the given groups in the network and the expected fraction if edges were randomly distributed. Modularity is used as a measure of the module assignment's ability to maximize intra-modular connections while minimizing inter-modular connections.
- **Participation coefficient:** One minus the across-module sum of the squared ratio between the number of within-module connections a node makes and the total degree of the node. Participation coefficient is a measure of how diverse a node's inter-modular connections are, with one being the most diverse and zero being the least.
- **Hubert rand index:** The cophenetic correlation coefficient as defined in (Hubert and Baker, 1977). This index is a measure of the stability of modular assignments.

Following methods of prior work (Owen et al., 2013), with code in the open-source Brain Connectivity Toolbox (http://sites.google.com/site/bctnet), modular assignments of 10,000 random initial conditions were calculated for every connectivity matrix. The most frequently appearing modular assignments were chosen for the complete AgCC and TDC connectomes. For individual connectivity matrices, the mean and standard deviation of modularity values and participation coefficients were calculated. The mean Hubert rand index was calculated between 1) modular assignments for each individual connectome and the consensus connectome and 2) every pair of modular assignments for all individual connectomes.

2.4. Intra- and inter-hemispheric graph metrics: Analyses at the network, lobe, and node levels

Children with complete AgCC (n = 13), partial AgCC (n = 6), and TDC (n = 29) were included in these analyses. Three different levels (network, lobe, and node) of comparisons were made on intra- and inter-hemispheric connections among groups. Intra- and inter-hemispheric connectivity matrices were extracted from the whole-brain connectivity matrix by filtering out irrelevant connections. At the network level, mean degree, cost, characteristic path length, mean normalized betweenness, and global efficiency were calculated for each connectivity matrix. Because local efficiency is zero for inter-hemispheric connectivity matrices by definition, it was only calculated for intra-hemispheric connectivity matrices. Lobe-level metrics were obtained by pooling graph metrics of the individual nodes that belong to the same lobe according to the Brainnetome atlas, i.e., frontal, temporal, parietal, occipital, insular, limbic, or subcortical nuclei. Degree and normalized betweenness were used for node-level analyses because they are defined for individual nodes and can be averaged across subjects at every node. Graph metric differences between the TDC group and the two AgCC groups respectively were calculated at node level.

2.4.1. Microstructural property measures of the anterior and posterior commissures

Based on tractography data, the streamlines crossing the midline through the anterior and posterior commissures were tracked using a multiple ROI approach consisting of placing a bilateral ROI in para-sagittal slices in the topography of the anterior or posterior commissures (Tovar-Moll et al., 2014). ROIs were manually defined by overlaying each participant's FA map with the co-registered T1-weighted image (Siffredi et al., 2019). The resulting tracts were exported to TrackVis format for visualization and selection of the streamlines of interest, i.e., fibers crossing the midline through the anterior and the posterior commissures (Catani and De Schotten, 2008; Siffredi et al., 2021b). The number of streamlines and mean FA measures along these bundles were extracted.

2.4.2. Neurobehavioral measures

Associations between graph metrics of intra- and inter-hemispheric structural connectivity and neurobehavioral outcomes were examined in the AgCC and TDC groups. Five domains of neurobehavioral functioning were examined using clinical tests and parent-reported questionnaires; general cognitive functioning, short-term and working memory, executive and attentional functioning, learning and memory, and social functioning (measures listed in Supplementary Table S1). A total of 33 age-standardized scores were included in the Partial Least Squares Correlation analysis.

2.5. Statistical analyses

2.5.1. Study replication analyses: Individual structural connectome

To assess the difference between the individual structural connectomes of complete AgCC and TDC groups, as in the work by Owen and colleagues (2013), a non-parametric test of 5000 random permutations was applied to every graph metric. P-values were calculated from the distribution of t-values from the permutations and significance was determined with a threshold of $p < 0.05$ after Bonferroni correction to account for multiple comparisons.

2.5.2. Intra- and inter-hemispheric graph metrics: Analyses at the network, lobe, and node levels

Student's t-tests were applied to compare network and lobe-level individual structural connectome metrics of complete AgCC, partial AgCC, and TDC groups. Significance was determined with a threshold of $p < 0.05$ after Bonferroni correction. For node-level comparisons of intra- and inter-hemispheric mean degree and mean normalized betweenness, nodes with AgCC-TDC group differences that fell outside of the 95% confidence interval obtained with bootstrapping analysis (500 bootstrap samples with replacement) were identified as outliers.

2.5.3. Association of inter-hemispheric graph metrics and microstructural property measures of the anterior and posterior commissures

To explore the potential role of the anterior and posterior commissures in inter-hemispheric graph metrics, Pearson's correlations between inter-hemispheric graph metrics and microstructural property measures of the anterior and posterior commissures (i.e., number of streamlines and mean FA) were completed. These correlations were done separately in the TDC, the complete AgCC and the partial AgCC groups.

2.5.4. Associations of intra- and inter-hemispheric graph metrics with neurobehavioral measures

Partial Least Squares Correlation (PLSC) analyses were performed to evaluate associations between lobe-level structural connectivity graph metrics and neurobehavioral measures in the complete AgCC, partial AgCC and TDC groups. PLSC is a data-driven multivariate technique that maximizes the covariance between two matrices by identifying latent components (LCs), which are linear combinations of the two matrices (McIntosh and Lobaugh, 2004). A publicly available Matlab toolbox was used: https://github.com/danizoeller/myPLS (Zöller et al., 2019; Kebets et al., 2019). The graph metrics data were stored in a 48×28 matrix denoted X. Each row of X represents one subject and the matrix's 28 columns are made up of the four graph metrics (mean degree and mean normalized betweenness of intra- and inter-hemispheric connectivity respectively), with each metric calculated from the seven brain lobes of the Brainnetome atlas. The neurobehavioral data were gathered in a 48×33 matrix denoted Y, with each row matching one subject and each column one neurobehavioral score. A cross-covariance matrix R was calculated by $R = Y^T X$ for each group, concatenated, and then decomposed by singular value decomposition (SVD) as $R = U \Delta V^T$. Neurobehavioral saliences U and structural graph metrics saliences V were thus obtained, while Δ matrix contains singular values. Each column of U and V contains the neurobehavioral and brain patterns called "saliences" that characterize each LC. Each group had a separate set of neurobehavioral saliences, while structural graph metrics saliences were common for the three groups. The significance of LCs was determined by permutation testing (1000 permutations) with $p < 0.01$. Multiple comparisons were not controlled for this exploratory analysis. The stability of neurobehavioral and structural graph metrics saliences was assessed with bootstrapping (500 bootstrap samples with replacement). Following the PLSC interpretation in Krishnan et al. (2011), an absolute-valued bootstrapping Z-score larger than 1.96, which corresponds to a 95% confidence interval not crossing zero, is considered a stable contribution from each neurobehavioral and structural graph metrics salience.

3. Results

3.1. Sample characteristics

The characteristics of included participants in the AgCC and the TDC groups are presented in Table 1. 19 children with AgCC, including 13 with complete AgCC (isolated n = 4, complex n = 9) and 6 with partial AgCC (isolated n = 2, complex n = 4), as well as 29 TDC, were included in the present study, see Supplementary Table S2 for further clinical characteristics of the AgCC group.

3.2. Replication analyses

Compared with TDC, the consensus structural connectome of

Table 1
Characteristics of the participants from the AgCC and TDC groups.

	AgCC	TDC	Group comparison
n	19	29	–
Age in years, mean (SD)	11.9 (2.56)	11.75 (2.32)	$t(46) = 0.208$, $p = 0.836$
Age in years [range]	[8.67–17.08]	[8.00–16.42]	–
Sex, n	7 females, 12 males	13 females, 16 males	$X^2(1; 48) = 0.301$; $p = 0.583$
Handedness, n	11 R, 7 L, 1 M	26 R, 3 L	–
Full-Scale IQ, median	80.47	113.00	$W = 949$, $p < 0.001$
Full-Scale IQ [range]	[66–126]	[88–136]	–

Note: Full-scale IQ was measured using the Wechsler Abbreviated Intelligence Scale (WASI) or the Wechsler Intelligence Scale for Children, 4th edition (WISC-IV; n = 3) where the mean standardized score is M = 100 and SD = 15; Handedness was estimated using the Edinburgh Handedness Inventory where right-handed (R) = +40 to +100, left-handed (L) = −40 to −100, and mixed handed (M) = −40 to +40; Group comparisons were done using chi-square (X^2) for categorical variables, and independent sample *t*-test (t) or Wilcoxon signed-rank test (W, when assumptions for parametric tests were not respected) for continuous variables.

children with complete AgCC showed decreased mean degree, cost, and global efficiency, along with increased characteristic path length, mean normalized betweenness, and local efficiency (Supplementary Table S3). To assess the robustness of the results with respect to different thresholds, we re-analyzed the data in a range of threshold values from 25% to 65% with a step size of 5%. We were able to show that the original analysis results at 50% are robust and comparable with results obtained from averaging the graph metrics of consensus connectomes in the sizable range of threshold values. Individual structural connectome analyses showed the same trends with significant group differences in all graph metrics except for mean degree and cost (Supplementary Table S4). Our findings are thus comparable to those reported by Owen and colleagues (2013).

Modularity analyses were generally concordant with Owen and colleagues' (2013) findings. We also found significantly increased mean modularity, along with decreased mean participation coefficient and Hubert rand indices calculated from consensus connectomes and individual connectomes in children with complete AgCC compared with TDC (Supplementary Table S5). Further details on nodes and brain regions involved in different modules are provided in Supplementary Table S6.

3.3. Intra- and inter-hemispheric graph metrics

3.3.1. Network-level analyses

For intra-hemispheric metrics at the network level, complete and partial AgCC groups showed significant increases compared to TDC in mean degree, cost, and global efficiency, along with significant decreases in characteristic path length and mean normalized betweenness. Significant increase in local efficiency was observed in partial AgCC group (Fig. 1 and Supplementary Table S7). In contrast, the two AgCC groups showed significant reductions in all inter-hemispheric graph metrics compared with TDC, except in global efficiency. These differences remained statistically significant after Bonferroni correction. Notably, there were no significant differences between the complete and partial AgCC groups.

3.3.2. Lobe- and node-level analyses

For intra-hemispheric structural connectivity, the two AgCC groups showed significantly increased mean degree in the frontal, temporal, and insular lobes compared with TDC, and in the parietal lobe in children with complete AgCC compared with TDC (Fig. 2a, Supplementary Table S8). The increase in mean degree in the frontal lobe was more pronounced in children with partial than complete AgCC. In contrast, reduced intra-hemispheric mean degree was observed in the limbic and occipital lobes, and in subcortical regions. Differences in intra-hemispheric mean degree were also evident at the node level

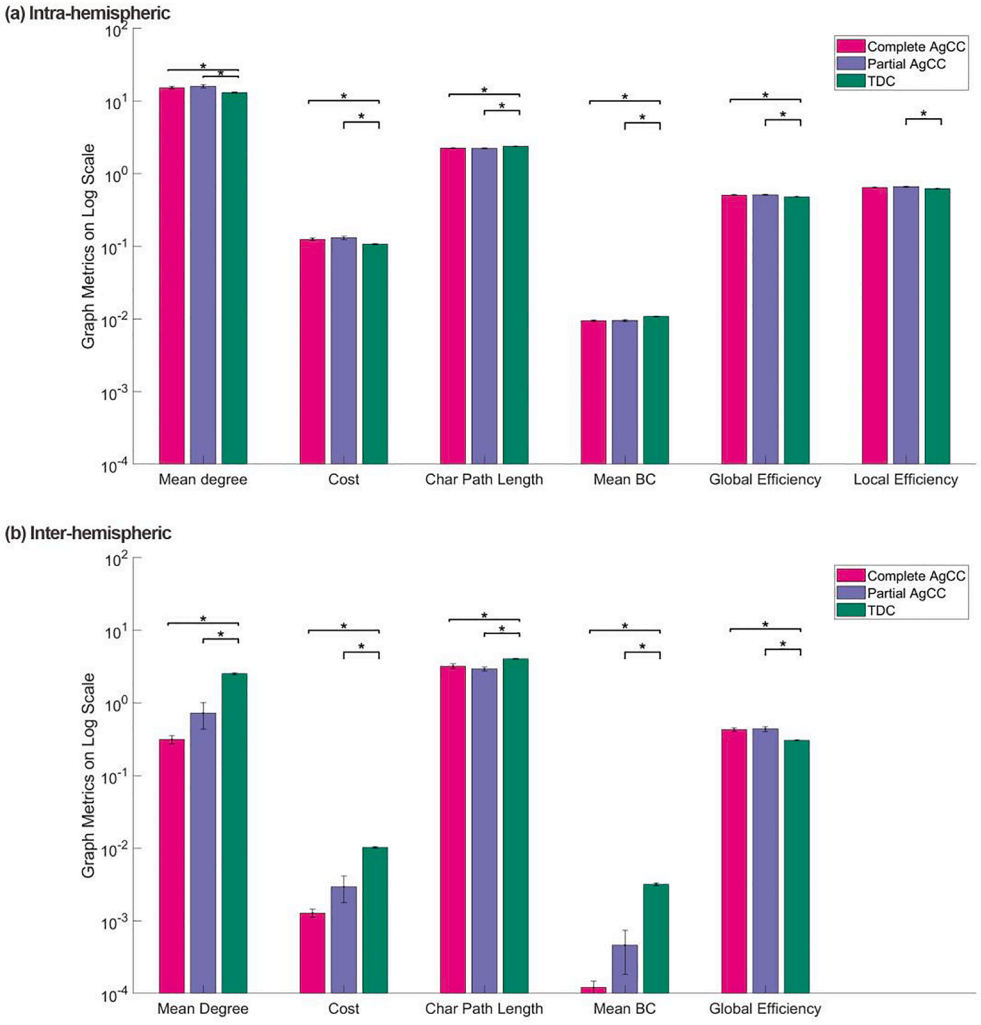

Fig. 1. Network-level intra-hemispheric (a) and inter-hemispheric (b) mean degree, cost, characteristic path length, mean normalized betweenness (BC), and global efficiency of complete AgCC, partial AgCC, and TDC groups. Plot is in log scale. * indicates statistical significance after Bonferroni correction at $p < 0.05$.

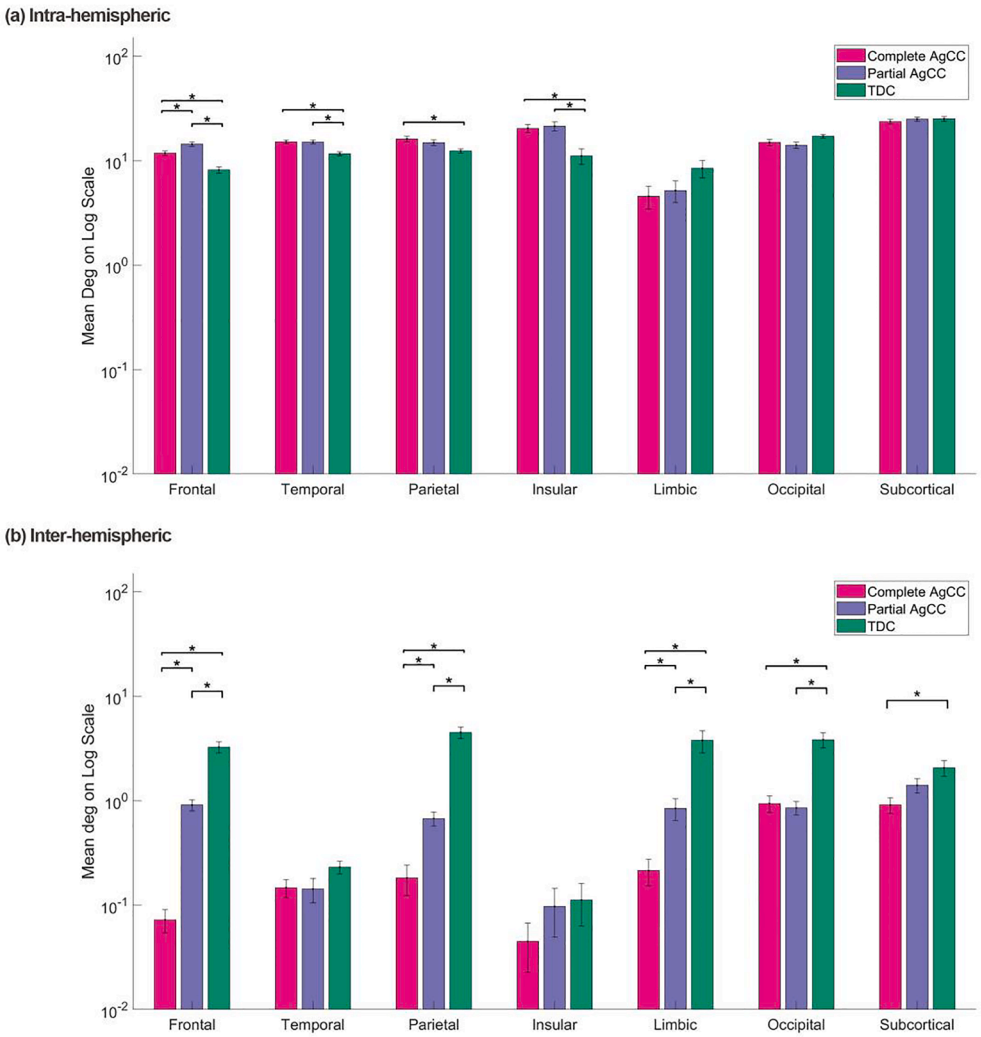

Fig. 2. Lobe-level intra-hemispheric (a) and inter-hemispheric (b) mean degree for complete AgCC, partial AgCC, and TDC groups. Plot is in log scale. * indicates statistical significance after Bonferroni correction at $p < 0.05$.

(Fig. 4a), with most nodes in frontal, parietal, insular, limbic, and occipital lobes showing higher mean degree in AgCC groups. Moreover, compared with other brain regions, insular and limbic lobes had nodes with mean degree differences that were less variable. For lobe-level intra-hemispheric mean normalized betweenness, no differences were found between complete AgCC, partial AgCC and TDC groups (Fig. 3a and Supplementary Table S9). At the node level, there were no clear differences in frontal, temporal, and parietal lobes between AgCC and TDC groups (Fig. 4a). Insular nodes had higher mean normalized betweenness in the AgCC group, while an opposite pattern was observed in limbic, occipital, and subcortical nodes. Regional variations were again observed, in particular most frontal, temporal, and parietal nodes had mean normalized betweenness differences centering around zero, with the last group of nodes showing more variations. All insular nodes in AgCC groups had higher mean normalized betweenness than the TDC group, while an opposite pattern was observed for nodes in occipital and subcortical lobes. For both graph metrics, the same outlier nodes were found in subcortical and parietal lobes in complete AgCC. In partial AgCC, outlier nodes for mean normalized betweenness also came from these brain regions, but those for mean degree came from occipital and insular lobes.

For inter-hemispheric structural connectivity, mean degree in both AgCC groups was generally reduced in all lobes with results reaching statistical significance in frontal, parietal, limbic, and occipital lobes (Fig. 2b). An additional reduction was seen in subcortical lobe for complete AgCC. Compared with partial AgCC, the reductions observed in the complete AgCC group were greater in frontal, parietal, and limbic lobes. These patterns were also reflected at the node level (Fig. 4b). For inter-hemispheric mean normalized betweenness at the lobe level, in the AgCC groups significant reductions were observed in frontal, parietal, limbic, occipital, and subcortical lobes (Fig. 3b). A reduction in frontal and parietal lobes was also observed in the complete AgCC compared with the partial AgCC group. At the node level, lower mean degree and mean normalized betweenness were observed in most of the nodes for the two AgCC groups. The exception was for nodes in temporal and insular lobes, where most nodes had similar mean normalized betweenness in the AgCC and TDC groups, with one outlier in the temporal node in each AgCC group. Additionally, both AgCC groups had outlier nodes from subcortical and limbic lobes for the two graph metrics respectively. For more details on node-level analysis, see Supplementary Tables S10–S12.

3.4. Comparisons between isolated and complex AgCC

For network level intra- and inter-hemispheric graph metrics, children with AgCC were grouped based on isolated AgCC (n = 6) or complex AgCC (n = 13), where AgCC is associated with other brain malformations. Network-level analyses show that none of the graph

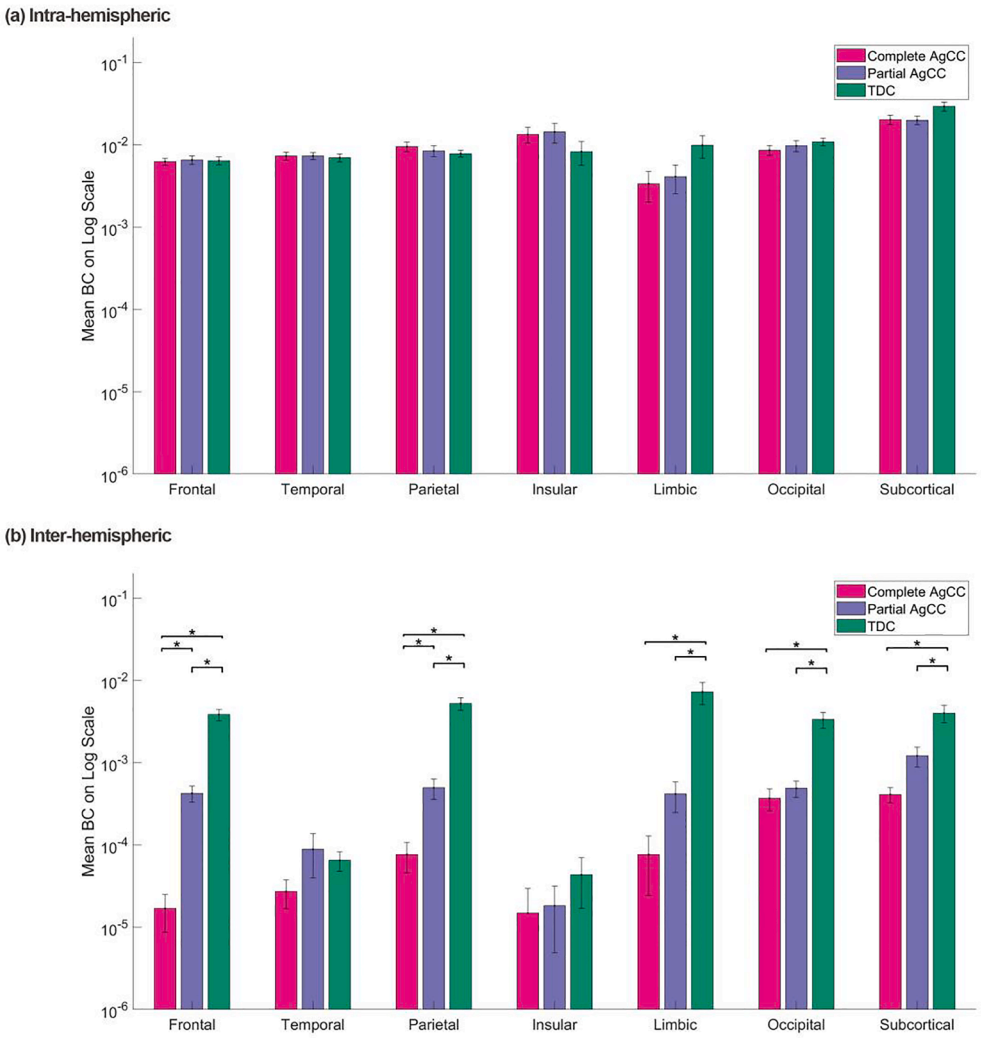

Fig. 3. Lobe-level intra-hemispheric (a) and inter-hemispheric (b) mean betweenness (BC) for complete AgCC, partial AgCC, and TDC groups. Plot is in log scale. * indicates statistical significance after Bonferroni correction at $p < 0.05$.

metrics differ significantly between the isolated and the complex AgCC groups, see Supplementary Table S13.

3.5. Associations between inter-hemispheric graph metrics and microstructural property measures of the anterior and posterior commissures

Pearson's correlation results are summarized in Supplementary Table S14. Notably, in complete AgCC it is observed that the mean FA of the anterior commissure, which is the mean FA along all the tracts crossing the midline via the anterior commissure, strongly and positively correlates with network-level inter-hemispheric mean degree, cost, and mean normalized betweenness (r greater than 0.7).

3.6. Associations between graph metrics and neurobehavioral measures

For neurobehavioral scores and group comparisons, see Supplementary Table S15. The PLSC analyses on lobe-level graph metrics and neurobehavioral measures in the complete AgCC, partial AgCC, and TDC groups identified two statistically significant LCs: LC1 ($p = 0.002$) and LC2 ($p = 0.002$), which explained 22.1% and 16.8% of the covariance between structural connectivity and neurobehavioral measures, respectively.

There were no clear patterns of association between the five neurobehavioral domains and the intra- and inter-hemispheric structural graph metrics in the AgCC nor TDC groups, see Fig. 5, Supplementary Figs. S2 and S3 and Tables S16 and S17. For LC1, robust saliences were found in verbal memory (i.e., scores of verbal delayed recall) and executive and attentional measures, including mostly processing speed, associated with both intra- and inter-hemispheric graph metrics in the TDC group only. Similarly, LC2 showed robust associations between intra- and inter-hemispheric graph measures and verbal scores in general, including learning and memory as well as switching in the TDC group mostly; and with the verbal immediate recall measure only in the complete AgCC group.

4. Discussion

The findings of this study shed light on the neuroplastic responses linked to intra- and inter- hemispheric structural organization in AgCC. First, following the same methodology as Owen and colleagues (Owen et al., 2013), we replicated their findings in a larger developmental cohort through extraction of comparable whole-brain graph metrics and modularity measures. In addition, we analyzed graph metrics within and across hemispheres to explore the hypothesis of structural strengthening of intra-hemispheric pathways in children with AgCC at different scales. Our network-level findings were consistent with this hypothesis as evidenced by the observed increases in fiber density as well as in network

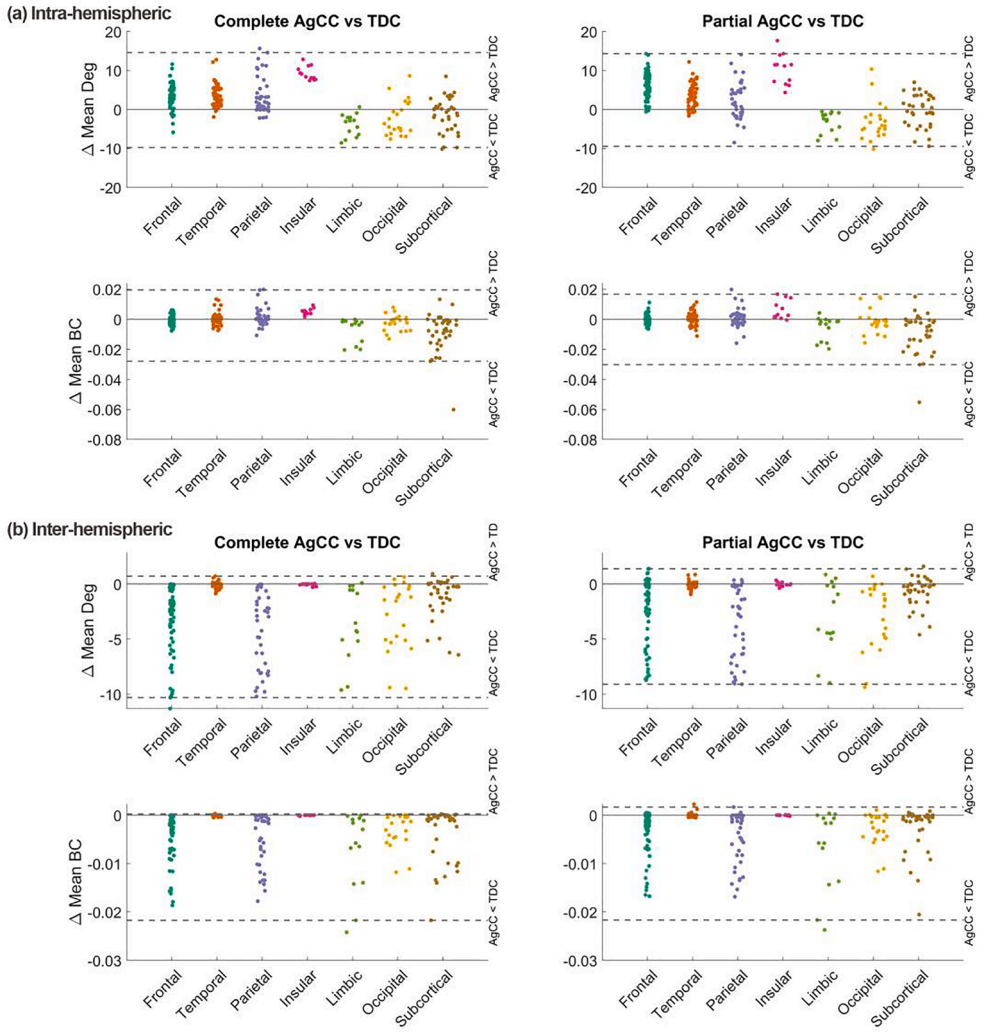

Fig. 4. Node-level mean degree and mean normalized betweenness (BC) differences between complete AgCC and TDC groups (left column) and between partial AgCC and TDC groups (right column) for (a) intra-hemispheric and (b) inter-hemispheric connections. In each plot solid lines indicate zero difference so that data points above 0 indicate higher metrics for the AgCC compared with TDC group and data points below 0 indicate higher metrics for the TDC group. Dashed lines show the 95% confidence interval from the bootstrapping analysis.

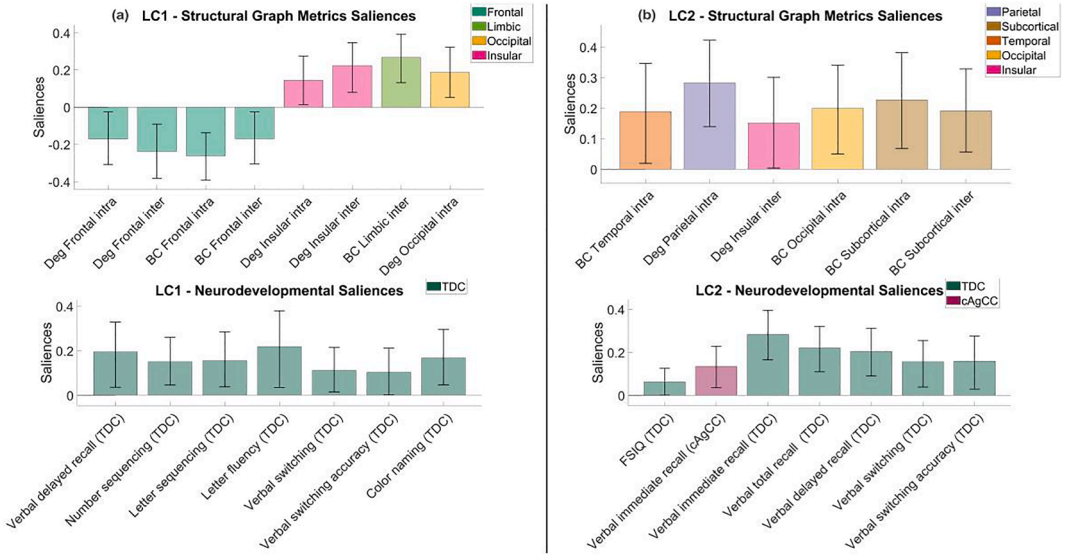

Fig. 5. Robust saliences of intra- and inter-hemispheric structural graph metrics (i.e., lobe level mean degree (Deg) and mean normalized betweenness (BC)) and neurobehavioral measures of (a) LC1 and (b) LC2 from PLSC analyses for complete AgCC (cAgCC), partial AgCC (pAgCC) and TDC. Note that only saliences with an absolute valued bootstrapping Z-score larger than 1.96, which corresponds to a 95% confidence interval not crossing zero, are considered stable contributions and are reported in this Figure.

local and global efficiency, along with a general decrease in inter-hemispheric graph metrics. Exploration of intra- and inter-hemispheric connections at the lobe and node levels allowed for characterizations of regional differences in structural connectivity in children with AgCC compared with TDC. Of further interest, we did not find evidence for associations between intra- and inter-hemispheric graph properties and neurobehavioral outcomes across a wide range of domains in this clinical population or in typically developing children.

Using similar graph theoretical analysis, we replicated the results of Owen and colleagues' (2013). Indeed, we found increased local connectivity graph metrics (i.e., local efficiency, clustering coefficient) in children with complete AgCC, and decreased global connectivity graph metrics (i.e., degree, cost, characteristic path length, normalized betweenness, and global efficiency). Modularity analyses revealed the same pattern, despite some differences in modular organization. Specifically, both Owen and colleagues (2013) and our current study have found increased mean modularity and decreased mean participation coefficient in children with complete AgCC. Additionally, the two studies showed a few differences in module assignment across the complete AgCC group, with more consistent modules in anterior parts of the brain, and more inconsistency in posterior areas (parietal, limbic, and occipital lobes). These small discrepancies in modularity analyses between the two studies are likely due to differences in parcellation. Together, our replication serves to validate and provide confidence in the representativeness of our data and clinical cohort.

Overall, our network-level findings were consistent with the hypothesis of structural strengthening of intra-hemispheric pathways in children with AgCC. For intra-hemispheric connections, both the complete and partial AgCC groups showed not only increased fiber density (i.e., mean degree, cost), but also strengthened overall structural connectivity (i.e., network global efficiencies) compared with TDC. Significantly stronger short-range structural connectivity (i.e., network local efficiencies) was also observed in partial AgCC. Conversely, all graph metrics were reduced for inter-hemispheric connections in children with complete and partial AgCC compared with TDC. Notably, there was an exception for inter-hemispheric global efficiency, which showed a significant increase in the AgCC groups compared with TDC. It is possible that these results reflect compensatory mechanisms, with the remaining inter-hemispheric structural connections being organized in a highly efficient way in children with AgCC. Consistent with these findings, other commissural structures, in particular the anterior commissure, have been proposed as alternative pathways for inter-hemispheric communication in the case of callosal alteration in humans (Siffredi et al., 2021b, 2019; Hung et al., 2019; Tovar-Moll et al., 2014) and in rhesus monkeys (O'Reilly et al., 2013). The strong positive correlations observed in our results between the mean FA of the anterior commissure and the network-level inter-hemispheric mean degree, cost, and mean normalized betweenness in complete AgCC are in line with this hypothesis.

When exploring intra- and inter-hemispheric connections at the lobe and node levels, structural connectivity changes in AgCC were found to vary spatially. Compared with TDC, children with complete and partial AgCC showed increased intra-hemispheric fiber density (i.e., mean degree) in frontal, temporal, parietal, and insular lobes, but not in the occipital lobe. It is possible that the increase observed in the parietal areas is composed of fibers from the Probst bundles. The Probst bundles are cortical fibers that fail to cross the midline and constitute in each cerebral hemisphere an aberrant longitudinal tract running in a rostro-caudal direction (Probst, 1901; Bénézit et al., 2015). The exception observed in occipital areas may also be attributed to the presence of colpocephaly, which is commonly observed in children with AgCC. Colpocephaly refers to enlarged occipital horns of the lateral ventricles, resulting in an atypical enlargement of the posterior or rear portion of the lateral ventricles, in the absence of the corpus callosum. Of particular interest, colpocephaly is known to affect structural connectivity in occipital regions (Aydin et al., 2016; Bartolome et al., 2016). Notably, no differences were observed for intra- hemispheric mean normalized betweenness suggesting typical structural connection centrality in complete and partial AgCC.

For inter-hemispheric lobe and node level graph metrics, decreased fiber density and centrality (i.e., mean degree and mean normalized betweenness) were found in the AgCC groups compared with TDC in several cortical structures that are normally connected inter-hemispherically by the corpus callosum, including frontal, parietal and occipital lobes. Findings at the node level revealed notable variations within these regions with node-level metrics differences spanning across large ranges. Temporal lobes showed comparable inter-hemispheric graph metrics between the AgCC and the TDC groups. The anterior commissure, mostly containing white matter fibers connecting bilateral temporal areas, probably plays a role in maintaining inter-hemispheric communication in these regions (Catani and De Schotten, 2008; Tovar-Moll et al., 2014; Siffredi et al., 2019, 2021b). Surprisingly, there was an overall reduction of fiber density and centrality measures for inter-hemispheric structural connectivity of subcortical and limbic areas in the AgCC groups compared with TDC. These findings are in contrast to the hypothesis that subcortical structures provide alternative pathways for interhemispheric communication, at least at the structural level (Mancuso et al., 2019). It is nevertheless possible that the observed decrease in subcortical fiber density and centrality measures is mostly attributed to the absent corpus callosum, whose effects overshadowed any countering effects in the remaining subcortical structures.

Finally, we observed several differences in connectivity for children with complete and partial AgCC. Children with partial AgCC had increased inter-hemispheric fiber density (i.e., mean degree) and betweenness centrality, as well as increased intra-hemispheric fiber density in the frontal lobe compared with children with complete AgCC. In partial AgCC, the remaining parts of the corpus callosum are mostly located anteriorly, including homotopic frontal structural connections (Siffredi et al., 2018). It is possible that by allowing callosal fibers to cross the midline in these restricted areas, the frontal lobes become a "hub" for the transfer of information across the brain in partial AgCC. Moreover, children with complete AgCC showed greater reductions in inter- hemispheric mean degree in parietal and limbic lobes compared with children with partial AgCC. Additionally, mean normalized betweenness in parietal lobes was further reduced in complete AgCC. This is again not surprising, as the remaining parts of the corpus callosum in partial AgCC also include homotopic parietal connections (Siffredi et al., 2018). Regarding limbic areas, it is possible that these structures are developing in a more typical way and are less affected by the absence of the corpus callosum in partial AgCC compared to complete AgCC.

Our investigation of associations between intra- and inter- hemispheric graph metrics at the lobe level and neurobehavioral outcomes across a wide range of domains did not identify any clear patterns of correlation in children with AgCC. Association between intra- and inter-hemispheric graph metrics and a few scores of verbal memory as well as executive and attentional measures were found in the TDC groups, but again without any clear pattern. These findings do not corroborate previous work showing an association between strengthening of structural intra-hemispheric connectivity and neurobehavioral outcomes in children with AgCC (Siffredi et al., 2021a). These discrepancies could be largely explained by the different measures of structural connectivity used in the two studies. Graph metrics in our study are primarily defined for binary systems and thus rely on the binarization of structural connectivity matrices, which are generated from the number of streamline measures and allow us to investigate the structural organization of the brain. Our choice of performing binary analysis is justified because most of the graph metrics calculations do not confer consistent or meaningful physical interpretation when extended to weighted structural connectome. Specifically, with the number of streamlines data as edge weights, connection strength is encoded rather than distance. Any

weighted graph metrics that deal with distance between nodes thus do not have proper meanings. These metrics include characteristic path length, normalized betweenness, global efficiency, and local efficiency (Yeh et al., 2020). Out of the remaining metrics, cost and clustering coefficient can only be binary because they are based on presence or absence of connections, leaving only degree that can be analyzed properly on weighted structural connectome. While weighted approach may yield more granular metrics, for our dataset binary analysis is more appropriate as it enables inclusion of a variety of graph metrics. Conversely, in this previous study (Siffredi et al., 2021a), the authors used edge-weighted measures including both the number of streamlines as well as fractional anisotropy (FA) measures, which quantify connectivity strength (Huang and Ding, 2016). It is possible that metrics derived from weighted graphical models with a proper physical interpretation or other structural graph metrics, such as small-worldness, assortativity or hierarchy, might be more strongly associated to neurodevelopmental outcomes (Cao et al., 2013; Ray et al., 2014). These important clinical questions need to be further investigated in order to better understand neurobehavioral variability and how it is associated with brain measures in this population.

This study provides new insights into brain structural organization in children with AgCC and despite some limitations, these findings could inform future research. First, our cohort is heterogeneous in terms of corpus callosum agenesis (including children with complete or partial AgCC) and associated brain malformations (including children with isolated or complex AgCC) which enabled us to examine connectivity in the range of children who present with AgCC. A larger sample size, however, would allow further explorations of each phenotypic group, as well as factors that contribute to neurobehavioral outcomes. Secondly, the two DWI shells acquired in the context of this study and used for multi-shell analyses are different in terms of TR and TE. It is more appropriate to acquire the same parameters of the different shells when combining them in multi-shell DWI analyses. Nevertheless, as a sanity check, analyses completed on the single *b3000* shell show highly comparable findings, confirming the reliability of our results. Thirdly, as a future direction, the combination and extension of our findings in animal models could significantly improve our understanding of the mechanisms involved in neuroplastic responses. Finally, the use of high quality data, for example, MRI acquisition using ultra-high field 7 Tesla would allow a higher parcellation resolution and could reveal fine structural reorganization in subcortical regions that were not captured in the present study and might be of clinical significance.

4.1. Conclusion

To our knowledge, this study is the first to employ graph metrics at the whole-brain level, with a multi-scale investigation of intra- and inter-hemispheric structural connectivity in children with AgCC. Our approach allowed the exploration of neuroplastic responses, specifically the hypothesis of structural strengthening of intra-hemispheric pathways in children with absence of corpus callosum. The major finding of our study is in support of this hypothesis, showing increased fiber density, as well as increased local and global network efficiency for intra-hemipheric connections in children with AgCC compared with typically developing children. Regional differences in fiber density and centrality metrics were also highlighted at the lobe and node levels. These structural alterations, however, did not appear to be associated with a wide range of neurobehavioral outcomes in children with AgCC.

Our results not only highlight the importance of graph-based analyses for quantifying structural connectivity changes in clinical populations at multiple resolutions, but also open avenues for future research looking into neuroplastic responses through reorganization of white matter tracts in various brain regions. To further investigate neuroplasticity in individuals with AgCC, a similar graph-based approach can be applied to analyze functional connectivity and structure–function couplings.

Acknowledgements

We gratefully acknowledge the families who participated in this study and Kate Pope for her assistance in recruitment of the families. This study was supported by the Boninchi Foundation from the University of Geneva; the Victorian Government's Operational Infrastructure Support Program; and the Murdoch Children's Research Institute. Professor Amanda Wood is supported by a European Research Council Consolidator Fellowship [682734]. Associate Professor Richard Leventer is supported by a Melbourne Children's Clinician Scientist Fellowship. Professor Vicki Anderson was supported by the Australian National Health and Medical Research Council Senior Practitioner Fellowship.

Funding

The Boninchi Foundation from the University of Geneva; the Victorian Government's Operational Infrastructure Support Program; the Murdoch Children's Research Institute. European Research Council Consolidator Fellowship (682734 to A.W.); a Melbourne Children's Clinician Scientist Fellowship (to R.L.); the Australian National Health and Medical Research Council Senior Practitioner Fellowship (to V.A.).

Appendix A. Supplementary data

Supplementary data to this article can be found online at https://doi.org/10.1016/j.nicl.2021.102709.

References

Anderson, V., Spencer-Smith, M., Wood, A., 2011. Do children really recover better? Neurobehavioural plasticity after early brain insult. Brain 134, 2197–2221.
Aydin, A.G., Adigüzel, E., Aksoy, A., Acar, K., 2016. Partial corpus callosum agenesis and colpocephaly: a case report. Anatomy: Int. J. Exp. Clin. Anatomy 10.
Bartolome, E., Cottura, J., Britos, R.F., Dominguez, R., 2016. Asymptomatic colpocephaly and partial agenesis of corpus callosum. Neurologia (Barcelona, Spain) 31, 68–70.
Bullmore, E.T., Bassett, D.S., 2011. Brain graphs: graphical models of the human brain connectome. Ann. Rev. Clin. Psychol. 7, 113–140. https://doi.org/10.1146/annurev-clinpsy-040510-143934.
Bénézit, A., Hertz-Pannier, L., Dehaene-Lambertz, G., Monzalvo, K., Germanaud, D., Duclap, D., Guevara, P., Mangin, J.-F., Poupon, C., Moutard, M.-L., Dubois, J., 2015. Organising white matter in a brain without corpus callosum fibres. Cortex 63, 155–171. https://doi.org/10.1016/j.cortex.2014.08.022.
Cao, Q., Shu, N., An, L., Wang, P., Sun, L., Xia, M.-R., Wang, J.-H., Gong, G.-L., Zang, Y.-F., Wang, Y.-F., et al., 2013. Probabilistic diffusion tractography and graph theory analysis reveal abnormal white matter structural connectivity networks in drug-naive boys with attention deficit/hyperactivity disorder. J. Neurosci. 33, 10676–10687.
Catani, M., De Schotten, M.T., 2008. A diffusion tensor imaging tractography atlas for virtual in vivo dissections. Cortex 44, 1105–1132.
Chiarello, C., 1980. A house divided? cognitive functioning with callosal agenesis. Brain Language 11, 128–158.
Dennis, M., 1976. Impaired sensory and motor differentiation with corpus callosum agenesis: a lack of callosal inhibition during ontogeny? Neuropsychologia 14, 455–469.
Dennis, M., Spiegler, B.J., Juranek, J.J., Bigler, E.D., Snead, O.C., Fletcher, J.M., 2013. Age, plasticity, and homeostasis in childhood brain disorders. Neurosci. Biobehav. Rev. 37, 2760–2773.
Fan, L., Li, H., Zhuo, J., Zhang, Y., Wang, J., Chen, L., Yang, Z., Chu, C., Xie, S., Laird, A. R., et al., 2016. The human brainnetome atlas: a new brain atlas based on connectional architecture. Cerebral Cortex 26, 3508–3526.
Grayson, D. S., Ray, S., Carpenter, S., Iyer, S., Dias, T. G. C., Stevens, C., Nigg, J. T., & Fair, D. A (2014). Structural and Functional Rich Club Organization of the Brain in Children and Adults. PLoS ONE, 9, e88297. doi:10.1371/journal.pone.0088297.
Huang, H., Ding, M., 2016. Linking functional connectivity and structural connectivity quantitatively: a comparison of methods. Brain Connectivity 6, 99–108.
Hubert, L.J., Baker, F.B., 1977. The comparison and fitting of given classification schemes. J. Math. Psychol. 16, 233–253. https://doi.org/10.1016/0022-2496(77)90054-2.
Hung, S.-C., Lee, C.-C., Chen, H.-H., Chen, C., Wu, H.-M., Lin, C.-P., Peng, S.-J., 2019. Early recovery of interhemispheric functional connectivity after corpus callosotomy. Epilepsia 60, 1126–1136.
Kebets, V., Holmes, A.J., Orban, C., Tang, S., Li, J., Sun, N., Kong, R., Poldrack, R.A., Yeo, B.T., 2019. Somatosensory-motor dysconnectivity spans multiple transdiagnostic dimensions of psychopathology. Biological Psychiatry 86, 779–791.

Krishnan, A., Williams, L.J., McIntosh, A.R., Abdi, H., 2011. Partial Least Squares (PLS) methods for neuroimaging: a tutorial and review. NeuroImage 56, 455–475. https://doi.org/10.1016/j.neuroimage.2010.07.034.

Mancuso, L., Uddin, L.Q., Nani, A., Costa, T., Cauda, F., 2019. Brain functional connectivity in individuals with callosotomy and agenesis of the corpus callosum: A systematic review. Neurosci. Biobehav. Rev. 105, 231–248.

McIntosh, A.R., Lobaugh, N.J., 2004. Partial least squares analysis of neuroimaging data: Applications and advances. Neuroimage 23, S250–S263.

Meoded, A., Katipally, R., Bosemani, T., Huisman, T.A.G.M., Poretti, A., 2015. Structural connectivity analysis reveals abnormal brain connections in agenesis of the corpus callosum in children. Eur. Radiol. 25, 1471–1478. https://doi.org/10.1007/s00330-014-3541-y.

Obertino, S., Hernández, S.J., Galazzo, I.B., Pizzini, F.B., Zucchelli, M., Menegaz, G., 2018. In: Exploiting machine learning principles for assessing the fingerprinting potential of connectivity features. Springer, pp. 175–188.

Owen, J.P., Li, Y.-O., Ziv, E., Strominger, Z., Gold, J., Bukhpun, P., Wakahiro, M., Friedman, E.J., Sherr, E.H., Mukherjee, P., 2013. The structural connectome of the human brain in agenesis of the corpus callosum. NeuroImage 70, 340–355. https://doi.org/10.1016/j.neuroimage.2012.12.031.

O'Reilly, J.X., Croxson, P.L., Jbabdi, S., Sallet, J., Noonan, M.P., Mars, R.B., Browning, P. G., Wilson, C.R., Mitchell, A.S., Miller, K.L., et al., 2013. Causal effect of disconnection lesions on interhemispheric functional connectivity in rhesus monkeys. Proc. Natl. Acad. Sci. 110, 13982–13987.

Paul, L.K., 2011. Developmental malformation of the corpus callosum: A review of typical callosal development and examples of developmental disorders with callosal involvement. J. Neurodevelopmental Disorders 3, 3–27. https://doi.org/10.1007/s11689-010-9059-y.

Paul, L.K., Brown, W.S., Adolphs, R., Tyszka, J.M., Richards, L.J., Mukherjee, P., Sherr, E. H., 2007. Agenesis of the corpus callosum: genetic, developmental and functional aspects of connectivity. Nature Rev. Neurosci. 8, 287–299. https://doi.org/10.1038/nrn2107. Number: 4 Publisher: Nature Publishing Group.

Probst, M., 1901. Uber den bau des vollstanding balkenlosen grobhirns. Arch Psychiatr 34, 709–786.

Ray, S., Miller, M., Karalunas, S., Robertson, C., Grayson, D.S., Cary, R.P., Hawkey, E., Painter, J.G., Kriz, D., Fombonne, E., et al., 2014. Structural and functional connectivity of the human brain in autism spectrum disorders and attention-deficit/hyperactivity disorder: A rich club-organization study. Human Brain Mapp. 35, 6032–6048.

Rubinov, M., Sporns, O., 2010. Complex network measures of brain connectivity: Uses and interpretations. NeuroImage 52, 1059–1069. https://doi.org/10.1016/j.neuroimage.2009.10.003.

Siffredi, V., Anderson, V., McIlroy, A., Wood, A.G., Leventer, R.J., Spencer-Smith, M.M., 2018. A neuropsychological profile for agenesis of the corpus callosum? cognitive, academic, executive, social, and behavioral functioning in school-age children. J. Int. Neuropsychol. Soc. 24, 445–455.

Siffredi, V., Preti, M.G., Kebets, V., Obertino, S., Leventer, R.J., McIlroy, A., Wood, A.G., Anderson, V., Spencer-Smith, M.M., Van De Ville, D., 2021a. Structural neuroplastic responses preserve functional connectivity through strengthening of intra-hemispheric pathways in children born without a corpus callosum. Cerebral Cortex 31 (2), 1227–1239.

Siffredi, V., Preti, M.G., Obertino, S., Leventer, R.J., Wood, A.G., McIlroy, A., Anderson, V., Spencer-Smith, M.M., Van De Ville, D., 2021b. Revisiting brain rewiring and plasticity in children born without corpus callosum. Develop. Sci. https://doi.org/10.1111/desc.13126.

Siffredi, V., Wood, A.G., Leventer, R.J., Vaessen, M., McIlroy, A., Anderson, V., Vuilleumier, P., Spencer-Smith, M.M., 2019. Anterior and posterior commissures in agenesis of the corpus callosum: Alternative pathways for attention processes? Cortex 121, 454–467.

Smith, R.E., Tournier, J.-D., Calamante, F., Connelly, A., 2013. Sift: Spherical-deconvolution informed filtering of tractograms. Neuroimage 67, 298–312.

Smith, S.M., 2002. Fast robust automated brain extraction. Human Brain Mapp. 17, 143–155.

Tax, C.M., Jeurissen, B., Vos, S.B., Viergever, M.A., Leemans, A., 2014. Recursive calibration of the fiber response function for spherical deconvolution of diffusion mri data. Neuroimage 86, 67–80.

J.-D. Tournier R. Smith D. Raffelt R. Tabbara T. Dhollander M. Pietsch D. Christiaens B. Jeurissen C.-H. Yeh A. Connelly Mrtrix3: A fast, flexible and open software framework for medical image processing and visualisation NeuroImage 2019 (p. 116137).

Tournier, J.-D., Yeh, C.-H., Calamante, F., Cho, K.-H., Connelly, A., Lin, C.-P., 2008. Resolving crossing fibres using constrained spherical deconvolution: validation using diffusion-weighted imaging phantom data. Neuroimage 42, 617–625.

Tovar-Moll, F., Monteiro, M., Andrade, J., Bramati, I.E., Vianna-Barbosa, R., Marins, T., Rodrigues, E., Dantas, N., Behrens, T.E., de Oliveira-Souza, R., et al., 2014. Structural and functional brain rewiring clarifies preserved interhemispheric transfer in humans born without the corpus callosum. Proc. Natl. Acad. Sci. 111, 7843–7848.

Yeh, C.-H., Jones, D.K., Liang, X., Descoteaux, M., Connelly, A., 2020. Mapping structural connectivity using diffusion MRI: Challenges and opportunities. J. Magn. Resonance Imag. https://doi.org/10.1002/jmri.27188. eprint: https://onlinelibrary.wiley.com/doi/pdf/10.1002/jmri.27188.

Yuan, J., Song, X., Kuan, E., Wang, S., Zuo, L., Ongur, D., Hu, W., Du, F., 2020. The structural basis for interhemispheric functional connectivity: Evidence from individuals with agenesis of the corpus callosum. NeuroImage: Clinical 28, 102425.

Zöller, D., Sandini, C., Karahanoğlu, F.I., Padula, M.C., Schaer, M., Eliez, S., Van De Ville, D., 2019. Large-scale brain network dynamics provide a measure of psychosis and anxiety in 22q11. 2 deletion syndrome. Biological Psychiatry: Cognitive Neurosci. Neuroimag. 4, 881–892.